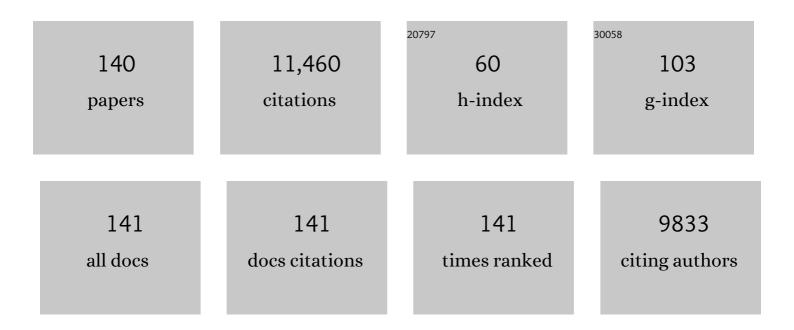
List of Publications by Year in descending order

Source: https://exaly.com/author-pdf/6988371/publications.pdf Version: 2024-02-01



#	Article	IF	CITATIONS
1	A Selfâ€Healable Sulfide/Polymer Composite Electrolyte for Longâ€Life, Lowâ€Lithiumâ€Excess Lithiumâ€Metal Batteries. Advanced Functional Materials, 2022, 32, 2106680.	7.8	28
2	Deciphering the exceptional kinetics of hierarchical nitrogen-doped carbon electrodes for high-performance vanadium redox flow batteries. Journal of Materials Chemistry A, 2022, 10, 5605-5613.	5.2	14
3	A detachable sandwiched polybenzimidazole-based membrane for high-performance aqueous redox flow batteries. Journal of Power Sources, 2022, 526, 231139.	4.0	14
4	Operating Highâ€Energy Lithiumâ€Metal Pouch Cells with Reduced Stack Pressure Through a Rational Lithiumâ€Host Design. Advanced Energy Materials, 2022, 12, .	10.2	10
5	Manipulation of Electrode Composition for Effective Water Management in Fuel Cells Fed with an Electrically Rechargeable Liquid Fuel. ACS Applied Materials & Interfaces, 2022, 14, 18600-18606.	4.0	5
6	Machine learning-assisted design of flow fields for redox flow batteries. Energy and Environmental Science, 2022, 15, 2874-2888.	15.6	23
7	A Nafion/polybenzimidazole composite membrane with consecutive proton-conducting pathways for aqueous redox flow batteries. Journal of Materials Chemistry A, 2022, 10, 13021-13030.	5.2	17
8	Anodeâ€Free Lithium–Sulfur Cells Enabled by Rationally Tuning Lithium Polysulfide Molecules. Angewandte Chemie, 2022, 134, .	1.6	5
9	Anodeâ€Free Lithium–Sulfur Cells Enabled by Rationally Tuning Lithium Polysulfide Molecules. Angewandte Chemie - International Edition, 2022, 61, .	7.2	13
10	A high-energy and long-cycling lithium–sulfur pouch cell via a macroporous catalytic cathode with double-end binding sites. Nature Nanotechnology, 2021, 16, 166-173.	15.6	392
11	A trifunctional electrolyte for high-performance zinc-iodine flow batteries. Journal of Power Sources, 2021, 484, 229238.	4.0	44
12	Elasticity-oriented design of solid-state batteries: challenges and perspectives. Journal of Materials Chemistry A, 2021, 9, 13804-13821.	5.2	12
13	A highly-efficient composite polybenzimidazole membrane for vanadium redox flow battery. Journal of Power Sources, 2021, 489, 229502.	4.0	29
14	Chloride ions as an electrolyte additive for high performance vanadium redox flow batteries. Applied Energy, 2021, 289, 116690.	5.1	30
15	Aligned microfibers interweaved with highly porous carbon nanofibers: A Novel electrode for high-power vanadium redox flow batteries. Energy Storage Materials, 2021, 43, 30-41.	9.5	35
16	Sodium–Sulfur Batteries Enabled by a Protected Inorganic/Organic Hybrid Solid Electrolyte. ACS Energy Letters, 2021, 6, 345-353.	8.8	34
17	A high-performance lithiated silicon–sulfur battery enabled by fluorinated ether electrolytes. Journal of Materials Chemistry A, 2021, 9, 25426-25434.	5.2	7
18	Highly catalytic hollow Ti3C2Tx MXene spheres decorated graphite felt electrode for vanadium redox flow batteries. Energy Storage Materials, 2020, 25, 885-892.	9.5	87

#	Article	IF	CITATIONS
19	A safe and efficient lithiated silicon-sulfur battery enabled by a bi-functional composite interlayer. Energy Storage Materials, 2020, 25, 217-223.	9.5	19
20	A high power density and long cycle life vanadium redox flow battery. Energy Storage Materials, 2020, 24, 529-540.	9.5	214
21	Towards uniform distributions of reactants via the aligned electrode design for vanadium redox flow batteries. Applied Energy, 2020, 259, 114198.	5.1	45
22	Enhanced cycle life of vanadium redox flow battery via a capacity and energy efficiency recovery method. Journal of Power Sources, 2020, 478, 228725.	4.0	33
23	Achieving multiplexed functionality in a hierarchical MXene-based sulfur host for high-rate, high-loading lithium-sulfur batteries. Energy Storage Materials, 2020, 33, 147-157.	9.5	64
24	On-Site Fluorination for Enhancing Utilization of Lithium in a Lithium–Sulfur Full Battery. ACS Applied Materials & Interfaces, 2020, 12, 53860-53868.	4.0	12
25	Asymmetric Porous Polybenzimidazole Membranes with High Conductivity and Selectivity for Vanadium Redox Flow Batteries. Energy Technology, 2020, 8, 2000592.	1.8	12
26	Flow Batteries: Modeling and Simulation of Flow Batteries (Adv. Energy Mater. 31/2020). Advanced Energy Materials, 2020, 10, 2070133.	10.2	26
27	Aligned hierarchical electrodes for high-performance aqueous redox flow battery. Applied Energy, 2020, 271, 115235.	5.1	28
28	Modeling and Simulation of Flow Batteries. Advanced Energy Materials, 2020, 10, 2000758.	10.2	66
29	An <i>in situ</i> encapsulation approach for polysulfide retention in lithium–sulfur batteries. Journal of Materials Chemistry A, 2020, 8, 6902-6907.	5.2	9
30	Balancing the specific surface area and mass diffusion property of electrospun carbon fibers to enhance the cell performance of vanadium redox flow battery. International Journal of Hydrogen Energy, 2020, 45, 12565-12576.	3.8	31
31	Rational design of spontaneous reactions for protecting porous lithium electrodes in lithium–sulfur batteries. Nature Communications, 2019, 10, 3249.	5.8	99
32	Investigation of an aqueous rechargeable battery consisting of manganese tin redox chemistries for energy storage. Journal of Power Sources, 2019, 437, 226918.	4.0	14
33	Artificial Bifunctional Protective layer Composed of Carbon Nitride Nanosheets for High Performance Lithium–Sulfur Batteries. Journal of Energy Storage, 2019, 26, 101006.	3.9	19
34	A gradient porous electrode with balanced transport properties and active surface areas for vanadium redox flow batteries. Journal of Power Sources, 2019, 440, 227159.	4.0	49
35	Mesoporous carbon derived from pomelo peel as a high-performance electrode material for zinc-bromine flow batteries. Journal of Power Sources, 2019, 442, 227255.	4.0	40
36	An aqueous manganese-copper battery for large-scale energy storage applications. Journal of Power Sources, 2019, 423, 203-210.	4.0	46

#	Article	IF	CITATIONS
37	A uniformly distributed bismuth nanoparticle-modified carbon cloth electrode for vanadium redox flow batteries. Applied Energy, 2019, 240, 226-235.	5.1	73
38	A bi-porous graphite felt electrode with enhanced surface area and catalytic activity for vanadium redox flow batteries. Applied Energy, 2019, 233-234, 105-113.	5.1	41
39	Mathematical modeling of the charging process of Li-S batteries by incorporating the size-dependent Li2S dissolution. Electrochimica Acta, 2019, 296, 954-963.	2.6	20
40	A room-temperature activated graphite felt as the cost-effective, highly active and stable electrode for vanadium redox flow batteries. Applied Energy, 2019, 233-234, 544-553.	5.1	59
41	Anion exchange membranes for aqueous acid-based redox flow batteries: Current status and challenges. Applied Energy, 2019, 233-234, 622-643.	5.1	101
42	An aqueous alkaline battery consisting of inexpensive all-iron redox chemistries for large-scale energy storage. Applied Energy, 2018, 215, 98-105.	5.1	40
43	Towards a uniform distribution of zinc in the negative electrode for zinc bromine flow batteries. Applied Energy, 2018, 213, 366-374.	5.1	83
44	Advances and challenges in alkaline anion exchange membrane fuel cells. Progress in Energy and Combustion Science, 2018, 66, 141-175.	15.8	388
45	Mn ₃ O ₄ Nanoparticleâ€Decorated Carbon Cloths with Superior Catalytic Activity for the V ^{II} /V ^{III} Redox Reaction in Vanadium Redox Flow Batteries. Energy Technology, 2018, 6, 1228-1236.	1.8	20
46	Borophene and defective borophene as potential anchoring materials for lithium–sulfur batteries: a first-principles study. Journal of Materials Chemistry A, 2018, 6, 2107-2114.	5.2	127
47	Improved electrolyte for zinc-bromine flow batteries. Journal of Power Sources, 2018, 384, 232-239.	4.0	100
48	Parameciumâ€Like Iron Oxide Nanotubes as a Costâ€Efficient Catalyst for Nonaqueous Lithiumâ€Oxygen Batteries. Energy Technology, 2018, 6, 263-272.	1.8	10
49	A Li ₂ Sâ€Based Sacrificial Layer for Stable Operation of Lithiumâ€Sulfur Batteries. Energy Technology, 2018, 6, 2210-2219.	1.8	4
50	Formation of electrodes by self-assembling porous carbon fibers into bundles for vanadium redox flow batteries. Journal of Power Sources, 2018, 405, 106-113.	4.0	54
51	Carbonized tubular polypyrrole with a high activity for the Br2/Brâ^' redox reaction in zinc-bromine flow batteries. Electrochimica Acta, 2018, 284, 569-576.	2.6	54
52	Highly efficient and ultra-stable boron-doped graphite felt electrodes for vanadium redox flow batteries. Journal of Materials Chemistry A, 2018, 6, 13244-13253.	5.2	97
53	Remedies of capacity fading in room-temperature sodium-sulfur batteries. Journal of Power Sources, 2018, 396, 304-313.	4.0	45
54	In-situ investigation of hydrogen evolution behavior in vanadium redox flow batteries. Applied Energy, 2017, 190, 1112-1118.	5.1	102

#	Article	IF	CITATIONS
55	A novel iron-lead redox flow battery for large-scale energy storage. Journal of Power Sources, 2017, 346, 97-102.	4.0	29
56	A stabilized high-energy Li-polyiodide semi-liquid battery with a dually-protected Li anode. Journal of Power Sources, 2017, 347, 136-144.	4.0	17
57	Ab initio prediction and characterization of phosphorene-like SiS and SiSe as anode materials for sodium-ion batteries. Science Bulletin, 2017, 62, 572-578.	4.3	61
58	High-performance zinc bromine flow battery via improved design of electrolyte and electrode. Journal of Power Sources, 2017, 355, 62-68.	4.0	111
59	High-performance nitrogen-doped titania nanowire decorated carbon cloth electrode for lithium-polysulfide batteries. Electrochimica Acta, 2017, 242, 137-145.	2.6	22
60	Critical transport issues for improving the performance of aqueous redox flow batteries. Journal of Power Sources, 2017, 339, 1-12.	4.0	154
61	A hydrogen-ferric ion rebalance cell operating at low hydrogen concentrations for capacity restoration of iron-chromium redox flow batteries. Journal of Power Sources, 2017, 352, 77-82.	4.0	42
62	A Lithium/Polysulfide Battery with Dual-Working Mode Enabled by Liquid Fuel and Acrylate-Based Gel Polymer Electrolyte. ACS Applied Materials & Interfaces, 2017, 9, 2526-2534.	4.0	24
63	Modeling of an aprotic Li-O2 battery incorporating multiple-step reactions. Applied Energy, 2017, 187, 706-716.	5.1	22
64	An aprotic lithium/polyiodide semi-liquid battery with an ionic shield. Journal of Power Sources, 2017, 342, 9-16.	4.0	15
65	Highly catalytic and stabilized titanium nitride nanowire array-decorated graphite felt electrodes for all vanadium redox flow batteries. Journal of Power Sources, 2017, 341, 318-326.	4.0	134
66	Highly active, bi-functional and metal-free B 4 C-nanoparticle-modified graphite felt electrodes for vanadium redox flow batteries. Journal of Power Sources, 2017, 365, 34-42.	4.0	75
67	A highly active biomass-derived electrode for all vanadium redox flow batteries. Electrochimica Acta, 2017, 248, 197-205.	2.6	53
68	An efficient Li2S-based lithium-ion sulfur battery realized by a bifunctional electrolyte additive. Nano Energy, 2017, 40, 240-247.	8.2	81
69	A self-cleaning Li-S battery enabled by a bifunctional redox mediator. Journal of Power Sources, 2017, 361, 203-210.	4.0	46
70	Boron phosphide monolayer as a potential anode material for alkali metal-based batteries. Journal of Materials Chemistry A, 2017, 5, 672-679.	5.2	217
71	Investigation and modeling of CPC based tubular photocatalytic reactor for scaled-up hydrogen production. International Journal of Hydrogen Energy, 2016, 41, 16019-16031.	3.8	25
72	Cost-effective carbon supported Fe2O3 nanoparticles as an efficient catalyst for non-aqueous lithium-oxygen batteries. Electrochimica Acta, 2016, 211, 545-551.	2.6	35

#	Article	IF	CITATIONS
73	A high-performance carbon nanoparticle-decorated graphite felt electrode for vanadium redox flow batteries. Applied Energy, 2016, 176, 74-79.	5.1	145
74	A low-cost iron-cadmium redox flow battery for large-scale energy storage. Journal of Power Sources, 2016, 330, 55-60.	4.0	44
75	Highly stable pyridinium-functionalized cross-linked anion exchange membranes for all vanadium redox flow batteries. Journal of Power Sources, 2016, 331, 452-461.	4.0	92
76	Ab initio prediction of a silicene and graphene heterostructure as an anode material for Li- and Na-ion batteries. Journal of Materials Chemistry A, 2016, 4, 16377-16382.	5.2	149
77	Two-dimensional SiS as a potential anode material for lithium-based batteries: A first-principles study. Journal of Power Sources, 2016, 331, 391-399.	4.0	46
78	Unraveling the Positive Roles of Point Defects on Carbon Surfaces in Nonaqueous Lithium–Oxygen Batteries. Journal of Physical Chemistry C, 2016, 120, 18394-18402.	1.5	50
79	Polyvinylpyrrolidone-based semi-interpenetrating polymer networks as highly selective and chemically stable membranes for all vanadium redox flow batteries. Journal of Power Sources, 2016, 327, 374-383.	4.0	46
80	In-situ Fabrication of a Freestanding Acrylate-based Hierarchical Electrolyte for Lithium-sulfur Batteries. Electrochimica Acta, 2016, 213, 871-878.	2.6	74
81	Copper nanoparticle-deposited graphite felt electrodes for all vanadium redox flow batteries. Applied Energy, 2016, 180, 386-391.	5.1	166
82	A highly permeable and enhanced surface area carbon-cloth electrode for vanadium redox flow batteries. Journal of Power Sources, 2016, 329, 247-254.	4.0	111
83	Performance enhancement of iron-chromium redox flow batteries by employing interdigitated flow fields. Journal of Power Sources, 2016, 327, 258-264.	4.0	93
84	A highly-safe lithium-ion sulfur polymer battery with SnO2 anode and acrylate-based gel polymer electrolyte. Nano Energy, 2016, 28, 97-105.	8.2	60
85	Facile preparation of high-performance MnO2/KB air cathode for Zn-air batteries. Electrochimica Acta, 2016, 222, 1438-1444.	2.6	26
86	The effects of design parameters on the charge-discharge performance of iron-chromium redox flow batteries. Applied Energy, 2016, 182, 204-209.	5.1	83
87	Computational insights into the effect of carbon structures at the atomic level for non-aqueous sodium-oxygen batteries. Journal of Power Sources, 2016, 325, 91-97.	4.0	21
88	Modeling of lithium-sulfur batteries incorporating the effect of Li2S precipitation. Journal of Power Sources, 2016, 336, 115-125.	4.0	87
89	A high-performance flow-field structured iron-chromium redox flow battery. Journal of Power Sources, 2016, 324, 738-744.	4.0	145
90	A high-performance dual-scale porous electrode for vanadium redox flow batteries. Journal of Power Sources, 2016, 325, 329-336.	4.0	157

#	Article	IF	CITATIONS
91	Borophene: A promising anode material offering high specific capacity and high rate capability for lithium-ion batteries. Nano Energy, 2016, 23, 97-104.	8.2	454
92	Novel gel polymer electrolyte for high-performance lithium–sulfur batteries. Nano Energy, 2016, 22, 278-289.	8.2	382
93	First-Principles Study of Nitrogen-, Boron-Doped Graphene and Co-Doped Graphene as the Potential Catalysts in Nonaqueous Li–O ₂ Batteries. Journal of Physical Chemistry C, 2016, 120, 6612-6618.	1.5	161
94	A nano-structured RuO ₂ /NiO cathode enables the operation of non-aqueous lithium–air batteries in ambient air. Energy and Environmental Science, 2016, 9, 1783-1793.	15.6	142
95	Modeling of anisotropic flow and thermodynamic properties of magnetic nanofluids induced by external magnetic field with varied imposing directions. Journal of Applied Physics, 2015, 118, .	1.1	34
96	Study on particle and photonic flux distributions in a magnetically stirred photocatalytic reactor. Journal of Photonics for Energy, 2015, 5, 052097.	0.8	3
97	A high-performance supportless silver nanowire catalyst for anion exchange membrane fuel cells. Journal of Materials Chemistry A, 2015, 3, 1410-1416.	5.2	73
98	A novel solid-state Li–O ₂ battery with an integrated electrolyte and cathode structure. Energy and Environmental Science, 2015, 8, 2782-2790.	15.6	111
99	A high-performance sandwiched-porous polybenzimidazole membrane with enhanced alkaline retention for anion exchange membrane fuel cells. Energy and Environmental Science, 2015, 8, 2768-2774.	15.6	59
100	Physicochemical properties of alkaline doped polybenzimidazole membranes for anion exchange membrane fuel cells. Journal of Membrane Science, 2015, 493, 340-348.	4.1	77
101	A modified aggregation based model for the accurate prediction of particle distribution and viscosity in magnetic nanofluids. Powder Technology, 2015, 283, 561-569.	2.1	40
102	Carbon-neutral sustainable energy technology: Direct ethanol fuel cells. Renewable and Sustainable Energy Reviews, 2015, 50, 1462-1468.	8.2	235
103	Fundamental models for flow batteries. Progress in Energy and Combustion Science, 2015, 49, 40-58.	15.8	133
104	A high-rate and long cycle life solid-state lithium–air battery. Energy and Environmental Science, 2015, 8, 3745-3754.	15.6	129
105	A comparative study of all-vanadium and iron-chromium redox flow batteries for large-scale energy storage. Journal of Power Sources, 2015, 300, 438-443.	4.0	251
106	A RuO ₂ nanoparticle-decorated buckypaper cathode for non-aqueous lithium–oxygen batteries. Journal of Materials Chemistry A, 2015, 3, 19042-19049.	5.2	40
107	A transient electrochemical model incorporating the Donnan effect for all-vanadium redox flow batteries. Journal of Power Sources, 2015, 299, 202-211.	4.0	52
108	A vanadium redox flow battery model incorporating the effect of ion concentrations on ion mobility. Applied Energy, 2015, 158, 157-166.	5.1	118

#	Article	IF	CITATIONS
109	Discharge product morphology versus operating temperature in non-aqueous lithium-air batteries. Journal of Power Sources, 2015, 278, 133-140.	4.0	36
110	The use of polybenzimidazole membranes in vanadium redox flow batteries leading to increased coulombic efficiency and cycling performance. Electrochimica Acta, 2015, 153, 492-498.	2.6	177
111	A low-cost, high-performance zinc–hydrogen peroxide fuel cell. Journal of Power Sources, 2015, 275, 831-834.	4.0	38
112	Modeling of lithium–oxygen batteries with the discharge product treated as a discontinuous deposit layer. Journal of Power Sources, 2015, 273, 440-447.	4.0	39
113	A high-performance ethanol–hydrogen peroxide fuel cell. RSC Advances, 2014, 4, 65031-65034.	1.7	32
114	Performance of a vanadium redox flow battery with and without flow fields. Electrochimica Acta, 2014, 142, 61-67.	2.6	125
115	A micro-porous current collector enabling passive direct methanol fuel cells to operate with highly concentrated fuel. Electrochimica Acta, 2014, 139, 7-12.	2.6	34
116	Nonequilibrium scheme for computing the flux of the convection-diffusion equation in the framework of the lattice Boltzmann method. Physical Review E, 2014, 90, 013305.	0.8	50
117	A gradient porous cathode for non-aqueous lithium-air batteries leading to a high capacity. Electrochemistry Communications, 2014, 46, 111-114.	2.3	54
118	Determination of the mass-transport properties of vanadium ions through the porous electrodes of vanadium redox flow batteries. Physical Chemistry Chemical Physics, 2013, 15, 10841.	1.3	54
119	Graphene sheets fabricated from disposable paper cups as a catalyst support material for fuel cells. Journal of Materials Chemistry A, 2013, 1, 183-187.	5.2	49
120	Numerical investigations of flow field designs for vanadium redox flow batteries. Applied Energy, 2013, 105, 47-56.	5.1	264
121	Preparation of silica nanocomposite anion-exchange membranes with low vanadium-ion crossover for vanadium redox flow batteries. Electrochimica Acta, 2013, 105, 584-592.	2.6	113
122	Mesoporous carbon with uniquely combined electrochemical and mass transport characteristics for polymer electrolyte membrane fuel cells. RSC Advances, 2013, 3, 16-24.	1.7	60
123	Prediction of the theoretical capacity of non-aqueous lithium-air batteries. Applied Energy, 2013, 109, 275-282.	5.1	48
124	Non-precious Co3O4 nano-rod electrocatalyst for oxygenreduction reaction in anion-exchange membranefuelcells. Energy and Environmental Science, 2012, 5, 5333-5339.	15.6	487
125	Charge carriers in alkaline direct oxidation fuel cells. Energy and Environmental Science, 2012, 5, 7536.	15.6	63
126	An alkaline direct ethanol fuel cell with a cation exchange membrane. Energy and Environmental Science, 2011, 4, 2213.	15.6	85

#	Article	IF	CITATIONS
127	High performance of a carbon supported ternary PdIrNi catalyst for ethanol electro-oxidation in anion-exchange membrane direct ethanol fuel cells. Energy and Environmental Science, 2011, 4, 1428.	15.6	101
128	Alkaline direct oxidation fuel cell with non-platinum catalysts capable of converting glucose to electricity at high power output. Journal of Power Sources, 2011, 196, 186-190.	4.0	128
129	Recent progress in understanding of coupled heat/mass transport and electrochemical reactions in fuel cells. International Journal of Energy Research, 2011, 35, 15-23.	2.2	9
130	Anion-exchange membrane direct ethanol fuel cells: Status and perspective. Frontiers of Energy and Power Engineering in China, 2010, 4, 443-458.	0.4	89
131	Density Functional Theory Studies of the Structure Sensitivity of Ethanol Oxidation on Palladium Surfaces. Journal of Physical Chemistry C, 2010, 114, 10489-10497.	1.5	92
132	Mass transport phenomena in direct methanol fuel cells. Progress in Energy and Combustion Science, 2009, 35, 275-292.	15.8	214
133	New DMFC Anode Structure Consisting of Platinum Nanowires Deposited into a Nafion Membrane. Journal of Physical Chemistry C, 2007, 111, 8128-8134.	1.5	71
134	Simulation of fluid flows in the nanometer: kinetic approach and molecular dynamic simulation. International Journal of Computational Fluid Dynamics, 2006, 20, 361-367.	0.5	15
135	A LATTICE BOLTZMANN MODEL FOR CONVECTION HEAT TRANSFER IN POROUS MEDIA. Numerical Heat Transfer, Part B: Fundamentals, 2005, 47, 157-177.	0.6	239
136	Measurements of Heat Transfer Coefficients From Supercritical Carbon Dioxide Flowing in Horizontal Mini/Micro Channels. Journal of Heat Transfer, 2002, 124, 413-420.	1.2	257
137	A Lattice BGK Scheme with General Propagation. Journal of Scientific Computing, 2001, 16, 569-585.	1.1	52
138	Variations of Buoyancy-Induced Mass Flux From Single-Phase to Two-Phase Flow in a Vertical Porous Tube With Constant Heat Flux. Journal of Heat Transfer, 1999, 121, 646-652.	1.2	10
139	A Numerical Study of Laminar Reciprocating Flow in a Pipe of Finite Length. Flow, Turbulence and Combustion, 1997, 59, 11-25.	0.2	9
140	Oscillatory Heat Transfer in a Pipe Subjected to a Laminar Reciprocating Flow. Journal of Heat Transfer, 1996, 118, 592-597.	1.2	60